Hysteresis Compensation in Piezoelectric Actuator Positioning Control Based on the Uncertainty and Disturbance Estimator

Jinhao Chen, Beibei Ren and Qing-Chang Zhong

***Abstract*—Robust and precise control of piezoelectric actuators is quite challenging due to the existence of strong hysteresis nonlinearities. In this paper, a control strategy is proposed based on the uncertainty and disturbance estimator (UDE) to improve the performance of the positioning control of piezoelectric actuators. Compared to the existing hysteresis inversion based or other robust control strategies, the UDE-based controller can achieve excellent positioning precision without the knowledge of the bound and shape of hysteresis. Simulation results are presented to illustrate the effectiveness of the UDE-based controller, where the system dynamics of the piezoelectric actuator are characterized by a second order linear system preceded by a symmetric or an asymmetric generalized Prandtl-Ishlinskii (GPI) input hysteresis model. The extraordinary capability of the UDE-based controller is further demonstrated on other smart material-based actuators, e.g., magnetostrictive, shape memory alloys (SMA), where the hysteresis is characterized by a saturated GPI model.**

***Index Terms*—Piezoelectric actuator, hysteresis, generalized Prandtl-Ishlinskii (GPI), uncertainty and disturbance estimator (UDE), robust control.**

I. Introduction

PIEZOELECTRIC actuators are widely applied in both industrial and academic research, e.g., in nanopositioning stage, microrobotics, active vibration control etc. [1], [2], [3], [4], [5], [6], [7]. The popularity of piezoelectric actuators can be attributed to its inherent merits, including fast response, ultra-high resolution, high output force, large bandwidth, zero backlash and little heat generation [8].

Despite the advantages of piezoelectric actuators, they generally exhibit strong hysteresis effects in their output response [9], which might cause inaccuracies, oscillations and even instability in some closed-loop systems. Since the 1980s, it has been found that the hysteresis nonlinearities in charge-driven piezoelectric actuators are minimal [10], [11]. Therefore, the hysteresis effect can be eliminated or reduced by using a charge-driven approach or a capacitor insertion method [12]. In [13], [14], a new type of current and charge amplifier was proposed and analyzed. Nevertheless, this unique property of piezoelectric materials has not been widely used yet because it is difficult to drive highly capacitive loads with available charge/current amplifier [15].

Compared to the charge control method, the voltage control method is more widely applied in practical systems actuated by piezoelectric materials. Generally, most existing voltage control strategies will be either hysteresis model-based compensation or non-model-based compensation. For the first category, a suitable hysteresis model is needed for identifying the hysteresis behavior. Several phenomenological models have been proposed and widely used for piezoelectric actuator modeling, e.g., Preisach model [16], [17], Prandtl-Ishlinskii (PI) model [9], [18], [19], [20], [21] and Bouc-Wen model [2], [22]. Also, a polynomial-based hysteresis model is introduced in [23]. Typically, a corresponding inversion of the hysteresis model needs to be calculated for the compensation of hysteresis by feedforward control. The challenges with such approaches lie in the hysteresis modeling complexity and parameter sensitivity. It has been found that the hysteretic behaviors of smart materials might be be varying with time, temperature or some other ambient conditions [24]. In addition, some of the hysteresis models (e.g., Preisach model) are not analytically invertible [9], so only approximate inversions can be obtained. Thus, such inversion-based feedforward controllers are generally employed with other feedback controllers to achieve precision positioning. Liu et al. in [17] combined a hysteresis compensator based on the inversion of Preisach model with a PID controller to achieve robust control of piezoelectric actuator. For the second category, a robust controller is designed to handle the uncertainty or disturbance introduced to the nominal system by the hysteresis effect. In [2], Li et al. proposed a sliding mode control with disturbance estimation featured by a PID-based sliding surface and adaptive gains, which only requires online estimation of disturbance and control gains rather than the knowledge of bounds on uncertainties. Wu et al. in [25] introduced a H_∞ robust feedback control combined with feedforward control based on system inversion to achieve high-speed precision output tracking on the piezoelectric actuator. A fuzzy decentralized control approach was proposed and applied for trajectory tracking by Hwang [26]. Enlightened by [27], a dynamic surface control scheme is proposed for piezoelectric fuel injector [28].

Unlike those aforementioned robust but complex controllers designed for specified hysteresis (model or shape), the target of this paper is to introduce a more simplified and

Jinhao Chen and Beibei Ren are with the Department of Mechanical Engineering, Texas Tech University, Lubbock, TX 79409-1021, USA, e-mail: jinhao.chen@ttu.edu, beibei.ren@ttu.edu.

Qing-Chang Zhong is with the Department of Electrical and Computer Engineering, Illinois Institute of Technology, Chicago, IL 60616, USA, e-mail: zhongqc@iit.edu.

robust controller, which can mitigate the hysteresis effects of piezoelectric actuators modeled by various generalized Prandtl-Ishlinskii (GPI) hysteresis, including symmetric or asymmetric shape. To achieve this, an uncertainty and disturbance estimator (UDE)-based controller will be developed. The UDE is constructed based on an assumption that any signal can be recovered via a filter with the appropriate bandwidth [29]. In [30], the UDE-based controller was proved to be robust and applied to a class of nonlinear non-affine systems, and additionally the uncertainty and disturbance was well estimated. Such extraordinary capability of the UDE-based controller will be explored to alleviate the hysteresis effects of piezoelectric actuators in this paper.

The remainder of this paper is organized as follows. The preliminaries and problem formulation are given in Section II. In Section III, the UDE-based controller will be designed for piezoelectric actuators and the stability analysis of the closed-loop system will be given. Simulation results are provided in Section IV to verify the effectiveness of the proposed UDE-based control on the hysteresis compensation in piezoelectric actuators. In order to show the extraordinary capability of the UDE-based control, further study on the tracking control of other types of smart material-based actuators with saturated hysteresis, e.g., magnetostrictive, shape memory alloys (SMA), is presented in Section V. Conclusion will be made in Section VI.

II. Preliminaries and Problem Formulation

The linear dynamics of piezoelectric actuators are typically identified as a second-order linear system as follows:

$$\ddot{x}(t)+2\xi\omega_n\dot{x}(t)+\omega_n^2x(t) \quad = \quad \omega_n^2u(t), \tag{1}$$

where $x(t)$ is the system output (i.e., actuator displacement), and $u(t)$ is the excitation force generated by piezoelectric material deformation when the input voltage is applied. Due to the hysteresis effects in piezoelectric actuators, the relationship between the excitation force $u(t)$ and the input voltage $v(t)$ are usually nonlinear, which will be characterized by the generalized Prandtl-Ishlinskii (GPI) model in this paper.

A. Review on the GPI Hysteresis Model

The classic PI model integrates the classic play operator with a density function to describe the input-output hysteresis relationship. However, the nature of the classic play operator limits the capability of the classic PI model to characterize only symmetric hysteresis loops of piezoelectric actuators [19]. On the other hand, asymmetric hysteresis loops have been observed on some actuators using hard piezoelectric materials and saturated hysteresis loops also exist on some shape memory alloys (SMA) and magnetostrictive actuators [31]. To characterize such asymmetric hysteresis or saturated hysteresis, the GPI hysteresis model is proposed by introducing envelope functions to the classic play operator. Assume that the input signal $v(t)\in C[0,\ T)$ is monotonic on the subinterval $[t_i,t_{i+1}]$, $i=0,1,2,\cdots$, and $t_0=0$. Then the GPI hysteresis model can be represented as below [9]:

$$u(t)=H[v](t)=\int_0^D p(r)F_r[v](t)dr, \tag{2}$$

where r refers to the threshold value as $0=r_0<r_1<\cdots<r_n=D$; the density function $p(r)$ satisfies $p(r)\geqslant 0$ with $\int_0^\infty rp(r)dr<\infty$; D is a constant so that the density function $p(r)$ vanishes for r larger than D; the generalized play operator $F_r[v](t)$ is defined as

$$\begin{aligned} F_r[v](t) &= f_r(v(t),\ F_r[v](t_i)),\ \text{for } t_i<t<t_{i+1}, \\ F_r[v](0) &= f_r(v(0),0), \\ f_r(v,w) &= \max(\gamma_L(v)-r,\min(\gamma_R(v)+r,w)), \end{aligned}$$

where $\gamma_L(v)$ and $\gamma_R(v)$ are the aforementioned envelope functions. By choosing different envelope functions, the GPI model can be used to characterize various shapes of hysteresis. When $\gamma_L(v)=\gamma_R(v)=v$, the GPI model is reduced to the classic PI model, i.e., the classic PI model is a special case of GPI model. The asymmetric hysteresis loops can be characterized by using different $\gamma_L(v)$ and $\gamma_R(v)$, and the saturated hysteresis can be modeled by choosing the envelop functions, e.g., in the form of $a_0\tanh(a_1v+a_2)+a_3$, with $a_1,\ a_2,\ a_3$ as constants.

B. Problem Formulation

Define $\boldsymbol{X}(t)=[x_1(t)\ x_2(t)]^T=[x(t)\ \dot{x}(t)]^T$ as the state vector, then (1) can be re-expressed as

$$\begin{bmatrix} \dot{x}_1(t) \\ \dot{x}_2(t) \end{bmatrix} = \begin{bmatrix} 0 & 1 \\ -\omega_n^2 & -2\xi\omega_n \end{bmatrix} \begin{bmatrix} x_1(t) \\ x_2(t) \end{bmatrix} + \begin{bmatrix} 0 \\ \omega_n^2 \end{bmatrix} u(t). \tag{3}$$

Substituting the input hysteresis (2) into (3), the full dynamics model of the piezoelectric actuator can be obtained as

$$\dot{\boldsymbol{X}}(t)=\boldsymbol{A}\boldsymbol{X}(t)+\boldsymbol{B}H[v](t), \tag{4}$$

with $A=\begin{bmatrix} 0 & 1 \\ -\omega_n^2 & -2\xi\omega_n \end{bmatrix}$ and $B=\begin{bmatrix} 0 & \omega_n^2 \end{bmatrix}^T$. For the trajectory tracking task, the desired trajectory is specified by $\boldsymbol{X}_m(t)=[x_{1m}(t)\ x_{2m}(t)]^T=[x_m(t)\ \dot{x}_m(t)]^T$, which is assumed to be piecewise continuous and uniformly bounded. The control objective is to design the control signal $v(t)$ so that the tracking error $\boldsymbol{e}(t)=[e_1(t)\ e_2(t)]^T=\boldsymbol{X}_m(t)-\boldsymbol{X}(t)$ asymptotically converges to zero with the desired error dynamics governed by

$$\dot{\boldsymbol{e}}(t)=\boldsymbol{K}\boldsymbol{e}(t), \tag{5}$$

where $\boldsymbol{K}\in R^{2\times 2}$ is the error feedback gain matrix and chosen to be in the form of $\begin{bmatrix} 0 & 1 \\ -k_1 & -k_2 \end{bmatrix}$, with $k_1,k_2>0$.

III. Control Design and Stability Analysis

A. UDE-Based Controller Design

The UDE-based controller will be designed in this subsection for the tracking problem stated in Section II-B without knowing the dynamics and bound of hysteresis. To facilitate the control design, the dynamics model of piezoelectric actuators (4) is reformulated as

$$\begin{aligned}\dot{\boldsymbol{X}}(t) &= \boldsymbol{A}\boldsymbol{X}(t) + \boldsymbol{B}\cdot[v(t) + H[v](t) - v(t)] \\ &= \boldsymbol{A}\boldsymbol{X}(t) + \boldsymbol{B}\cdot v(t) + \boldsymbol{u}_d(v(t)),\end{aligned} \tag{6}$$

in which, the lumped vector $\boldsymbol{u}_d(v(t))$ includes the GPI hysteresis $H[v](t)$ and the control signal $v(t)$, i.e.,

$$\boldsymbol{u}_d(v(t)) \triangleq \boldsymbol{B}\cdot[H[v](t) - v(t)]. \tag{7}$$

Combining (5) and (6) results in

$$\dot{\boldsymbol{X}}_m(t) - [\boldsymbol{A}\boldsymbol{X}(t) + \boldsymbol{B}\cdot v(t) + \boldsymbol{u}_d(v(t))] = \boldsymbol{K}\boldsymbol{e}(t).$$

Thus, the control signal $v(t)$ should satisfy

$$\boldsymbol{B}v(t) = \dot{\boldsymbol{X}}_m(t) - \boldsymbol{A}\boldsymbol{X}(t) - \boldsymbol{u}_d(v(t)) - \boldsymbol{K}\boldsymbol{e}(t). \tag{8}$$

According to the system dynamics (6), the lumped uncertainty and disturbance term $\boldsymbol{u}_d(v(t))$ can be represented as

$$\boldsymbol{u}_d(v(t)) = \dot{\boldsymbol{X}}(t) - \boldsymbol{A}\boldsymbol{X}(t) - \boldsymbol{B}v(t).$$

This shows that the lumped term can be obtained from the known dynamics of the piezoelectric actuator and voltage input. However, the direct use of this relation will cause algebraic loops and the control law can not be formulated. In [29], Zhong and Rees derived the UDE-based robust controller by using the estimation of this lumped signal in the frequency domain. This is achievable because a signal can be recovered by passing it through a filter, of which the bandwidth is wide enough to cover the spectrum of that signal. According to the assumption in [29] that if the filter $G_f(s)$ is strictly stable and has the unity gain and zero phase shift over the spectrum of $\boldsymbol{u}_d(v(t))$ and zero gain elsewhere, then $\boldsymbol{u}_d(v(t))$ can be accurately represented by

$$\begin{aligned}\hat{\boldsymbol{u}}_d(v(t)) &= \boldsymbol{u}_d(v(t)) * g_f(t) \\ &= (\dot{\boldsymbol{X}}(t) - \boldsymbol{A}\boldsymbol{X}(t) - \boldsymbol{B}v(t)) * g_f(t),\end{aligned} \tag{9}$$

where "$*$" is the convolution operator and $g_f(t)$ is the impulse response of $G_f(s)$. This procedure is equivalent to amplify the signal $\boldsymbol{u}_d(v(t))$ by the gain 1 without shifting the phase for the frequency components that fall into the bandwidth of the filter $G_f(s)$, and at the same time, block anything outside the bandwidth of the filter $G_f(s)$, which is 0 anyway. Therefore, the signal is well represented without adding or losing any information. Replacing $\boldsymbol{u}_d(v(t))$ with $\hat{\boldsymbol{u}}_d(v(t))$ in (8) results in

$$\begin{aligned}\boldsymbol{B}v(t) &= \dot{\boldsymbol{X}}_m(t) - \boldsymbol{A}\boldsymbol{X}(t) - \boldsymbol{K}\boldsymbol{e}(t) \\ &\quad -(\dot{\boldsymbol{X}}(t) - \boldsymbol{A}\boldsymbol{X}(t) - \boldsymbol{B}v(t)) * g_f(t).\end{aligned} \tag{10}$$

By noting $\boldsymbol{B}v(t) = \boldsymbol{\phi}(t)$, then

$$\begin{aligned}\boldsymbol{\phi}(t) &= (\dot{\boldsymbol{X}}_m(t) - \boldsymbol{K}\boldsymbol{e}(t)) * \mathcal{L}^{-1}\left\{\frac{1}{1-G_f(s)}\right\} \\ &\quad -\boldsymbol{A}\boldsymbol{X}(t) - \boldsymbol{X}(t) * \mathcal{L}^{-1}\left\{\frac{sG_f(s)}{1-G_f(s)}\right\}\end{aligned} \tag{11}$$

where $\mathcal{L}^{-1}\{\cdot\}$ is the inverse operator of Laplace transform. It is noted that no approximation is made before this point, and (11) should satisfy (4).

By rewriting (10) as

$$\begin{aligned}&\begin{bmatrix} 0 \\ \omega_n^2 \end{bmatrix} v(t) \\ =\ &\begin{bmatrix} \dot{x}_m(t) \\ \ddot{x}_m(t) \end{bmatrix} - \begin{bmatrix} 0 & 1 \\ -\omega_n^2 & -2\xi\omega_n \end{bmatrix}\begin{bmatrix} x(t) \\ \dot{x}(t) \end{bmatrix} \\ &- \begin{bmatrix} 0 & 1 \\ -k_1 & -k_2 \end{bmatrix}\begin{bmatrix} e_1(t) \\ e_2(t) \end{bmatrix} \\ &- \left(\begin{bmatrix} \dot{x}(t) \\ \ddot{x}(t) \end{bmatrix} - \begin{bmatrix} 0 \\ \omega_n^2 \end{bmatrix} v(t)\right) * g_f(t) \\ &+ \left(\begin{bmatrix} 0 & 1 \\ -\omega_n^2 & -2\xi\omega_n \end{bmatrix}\begin{bmatrix} x(t) \\ \dot{x}(t) \end{bmatrix}\right) * g_f(t),\end{aligned}$$

it can be found that the first equation is always satisfied. That means the solution for the second equation [i.e., $\omega_n^2 \cdot v(t) = \begin{bmatrix} 0 & 1 \end{bmatrix}\boldsymbol{\phi}(t)$] which is unique, can be used as the controller to fulfill the trajectory tracking task. The UDE-based controller for piezoelectric actuator systems is then established in the following

$$v(t) = \begin{bmatrix} 0 & \frac{1}{\omega_n^2} \end{bmatrix}\boldsymbol{\phi}(t). \tag{12}$$

It is worth pointing out that no bound and other information of the hysteresis nonlinearities is needed for the UDE-based controller design.

B. Stability Analysis

The asymptotic stability of the closed-loop system is presented in the theorem below.

Theorem 1. *For a closed-loop system consisting of the dynamic model (4), the desired trajectory $X_m(t)$, and control law (11), if the filter $G_f(s)$ is chosen to be a strictly-proper stable with unity gain and zero phase shift over the spectrum of the lumped term $\boldsymbol{u}_d(v(t))$ and zero gain elsewhere, then the closed-loop system is asymptotically stable. Furthermore, the tracking error dynamics converge as governed by (5).*

Proof: If the lumped uncertainty and disturbance term $\boldsymbol{u}_d(v(t))$ is known, then substituting (8) into (6) will result in the desired error dynamics (5). However, without knowing $\boldsymbol{u}_d(v(t))$, the estimated term $\hat{\boldsymbol{u}}_d(v(t))$ from (9) is used to replace $\boldsymbol{u}_d(v(t))$. This brings the error dynamics in the form of

$$\dot{\boldsymbol{e}}(t) = \boldsymbol{K}\boldsymbol{e}(t) + \tilde{\boldsymbol{u}}_d(t), \tag{13}$$

where $\tilde{\boldsymbol{u}}_d(v(t)) := \boldsymbol{u}_d(v(t)) - \hat{\boldsymbol{u}}_d(v(t))$ is the estimation error of the lumped vector. Based on (9), the estimation error should be $\tilde{\boldsymbol{u}}_d(v(t)) = \boldsymbol{u}_d(v(t)) * \mathcal{L}^{-1}\{1 - G_f(s)\}$. Since the filter $G_f(s)$ is designed to be strictly proper and stable with unity gain and zero phase shift over the whole spectrum of $\boldsymbol{u}_d(v(t))$ and zero gain elsewhere, then $\tilde{\boldsymbol{u}}_d(v(t)) = 0$. Hence, the error dynamics (13) will converge to the desired dynamics (5), which is asymptotically stable. This completes the proof.

■

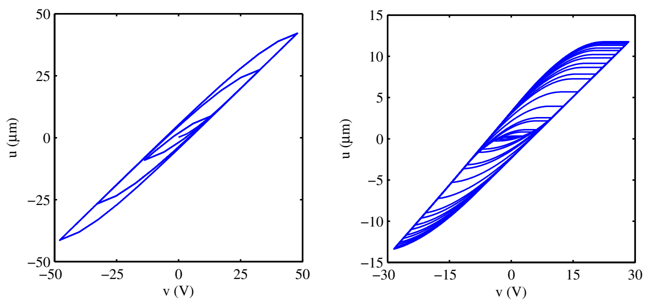

(a) $u = H_{sym}[v](t)$ (b) $u = H_{asym}[v](t)$

Figure 1. Symmetric and asymmetric GPI hysteresis loops.

IV. Simulation Results

In this section, simulation results will be provided to verify the effectiveness of the proposed UDE-based controller for the piezoelectric actuator model in (1) with $\omega_n = 50$ and $\xi = 0.5$. Thus, the system is identified as

$$\dot{\boldsymbol{X}}(t) = \begin{bmatrix} 0 & 1 \\ -2500 & -50 \end{bmatrix} \boldsymbol{X}(t) + \begin{bmatrix} 0 \\ 2500 \end{bmatrix} u(t),$$

where $u(t)$ is the GPI hysteresis output fed by the control signal $v(t)$. Additionally, the error feedback gain matrix is chosen as $\boldsymbol{K} = \begin{bmatrix} 0 & 1 \\ -8100 & -1800 \end{bmatrix}$. As mentioned in Section II-A, hysteresis effects in most piezoelectric actuators are symmetric, but asymmetric hysteresis effects also exist in some other piezoelectric actuators. Examples for these two different kinds of hysteresis characterized by the GPI model will be taken into consideration. In [9], the envelope functions in the forms of $\gamma_R(v) = c_{R0}v + c_{R1}$ and $\gamma_L(v) = c_{L0}v + c_{L1}$ are used to model both symmetric hysteresis and asymmetric hysteresis in piezoelectric actuators. The density function is chosen to be $p(r_i) = \rho e^{-\sigma r_i}$ with the threshold values $r_i = \alpha i,\ i = 0,\ 1,\ \cdots,\ N$. In particular, the parameters of symmetric hysteresis $H_{sym}[v](t)$ in a piezoelectric micropositioning stage (P-753.31 C) from the Physik Instrumente Company are identified as [9] $c_{R0} = c_{L0} = 0.89$, $c_{R1} = c_{L1} = 0.37$, $\alpha = 3.47$, $\rho = 0.54$, $\sigma = 0.16$ and $N = 9$. The parameters of asymmetric hysteresis $H_{asym}[v](t)$ are given as $c_{R0} = 1.2$, $c_{R1} = 1.9$, $c_{L0} = 1$, $c_{L1} = 0$, $\alpha = 0.24$, $\rho = 0.07$, $\sigma = 0.1$ and $N = 49$. The hysteresis loops of $H_{sym}[v](t)$ and $H_{asym}[v](t)$ are illustrated in Fig. 1 by using $v_1(t) = 30\sin(0.75\pi t) + 20\sin(0.5\pi t)$ (V) and $v_2(t) = 15\sin(2\pi t) + 13.5\cos(6t)$ (V) as the excitation signal respectively.

As noted in Section III, the filter $G_f(s)$ should have the unity gain on the spectrum of $\boldsymbol{u}_d(v(t))$ without phase shifting and zero gain outside the spectrum of to achieve the desired error dynamics. The following first-order low-pass filter is considered in the practice,

$$G_f(s) = \frac{1}{1+\tau s} \tag{14}$$

with the time constant τ. Though for such an approximated implementation of the filter specified in Theorem 1, UDE-based controller would lead to a non-zero but small estimation error $\tilde{\boldsymbol{u}}_d(t)$ and thus result in degraded performance, the performance could be excellent when a small enough τ is chosen such that the bandwidth of filter (14) is wide enough to cover most spectrum of $\boldsymbol{u}_d(v(t))$. In [32], some guidance of the filter design was provided by revealing the two-degree-of-freedom nature of the UDE-based controller. In practice, due to the limitations of sampling time Δt, τ can not be chosen as small as desired. Also, the filter with too wide bandwidth, when τ being too small, will introduce sensor noise with high frequency, and thus might degrade the performance of the UDE-based controller. Therefore, how to choose τ depends on the specified application including the hardware capability and the performance requirements. In our case, the acceptable range of τ is $[5\Delta t,\ 50\Delta t]$, with the sampling time $\Delta t = 0.001s$.

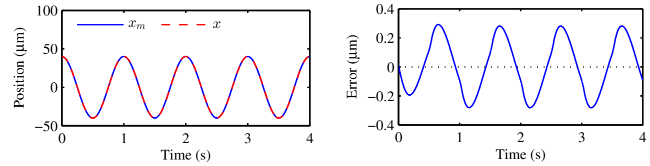

(a) Position $x(t)$ and its reference signal $x_m(t)$ (b) Tracking error

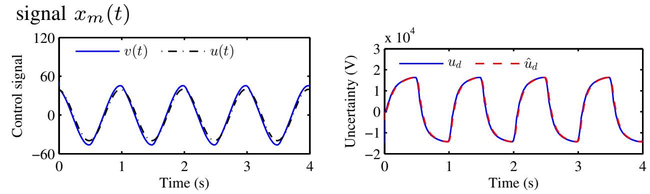

(c) Control signal $v(t)$ and hysteresis output $u(t)$ (d) Uncertainty $u_d(t)$ and its estimation $\hat{u}_d(t)$

Figure 2. Trajectory tracking performance of piezoelectric actuator with symmetric hysteresis.

By using such a filter (14), the following equations can be achieved

$$\frac{1}{1-G_f(s)} = 1 + \frac{1}{\tau s} \quad \text{and} \quad \frac{sG_f(s)}{1-G_f(s)} = \frac{1}{\tau}.$$

Therefore, the UDE-based controller can be further derived from (11) and (12) as

$$\begin{aligned} v(t) \quad = \quad & \frac{1}{2500}(\ddot{x}_m(t) + 8100e_1(t) + 1800e_2(t) + 50\dot{x}(t) \\ & +2500x(t)) + \frac{1}{2500\tau}(-\dot{x}(t) + \int_0^t (\ddot{x}_m(\xi) \\ & +8100e_1(\xi) + 1800e_2(\xi))d\xi). \end{aligned} \tag{15}$$

Other parameters are chosen as: the simulation time $4s$, and the filter parameter $\tau = 0.01s$. The desired trajectory is specified as $\boldsymbol{X}_m(t) = [x_m(t)\ \dot{x}_m(t)]^T$, $x_m(t) = M\cos(2\pi t)$ (μm) with the magnitude M. The initial states of the system are set to be $\boldsymbol{X}(0) = [M\,0]^T$. Due to different operation ranges of different actuators, the magnitudes of trajectories are set accordingly. Here, we set $M = 40$ for the

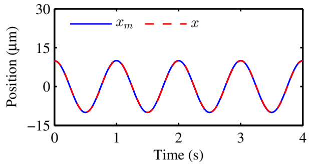

(a) Position $x(t)$ and its reference signal $x_m(t)$

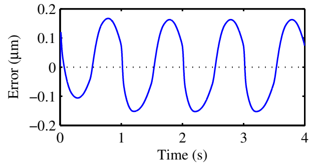

(b) Tracking error

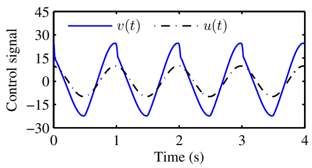

(c) Control signal $v(t)$ and hysteresis output $u(t)$

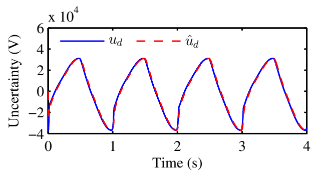

(d) Uncertainty $u_d(t)$ and its estimation $\hat{u}_d(t)$

Figure 3. Trajectory tracking performance of piezoelectric actuator with asymmetric hysteresis.

system with symmetric hysteresis $H_{sym}[v](t)$, and $M = 10$ for the system with asymmetric hysteresis $H_{asym}[v](t)$. The simulation results are presented in Figs. 2 and 3.

From Fig. 2(a), the system output can follow the desired output trajectory very well in the presence of a symmetric input hysteresis $H_{sym}[v](t)$. From Fig. 2(b), the tracking error is at most $0.29\mu m$, i.e., the relative tracking error is 0.7%. Due to the existence of hysteresis, it can be seen that the voltage input $v(t)$ and hysteresis output $u(t)$ are different in Fig. 2(c). The use of UDE keeps the uncertainty and disturbance lumped term $\boldsymbol{u}_d(v(t))$ being well estimated, as seen from Fig. 2(d). In this way, the lumped term $\boldsymbol{u}_d(v(t))$ can be compensated by the UDE-based controller to fulfill the trajectory tracking task successfully. It is noted that such a good performance is achieved by the proposed UDE-based controller (15) in the existence of hysteresis uncertainty $H_{sym}[v](t)$ but without the knowledge of its bound and shape.

Fig.3 shows the good trajectory tracking performance of the proposed UDE-based controller for piezoelectric actuators in the presence of asymmetric input hysteresis $H_{asym}[v](t)$. In this case, the tracking error is at most $0.17\mu m$, i.e., the relative tracking error is 1.7%. As shown in Fig.3(c), the difference between $v(t)$ and $u(t)$ is much larger than that in Fig. 2(c), which makes the hysteresis more difficult to compensate and control, and thus results in a little larger relative error.

V. Further Study on Saturated GPI Hysteresis Compensation

In Section IV, both symmetric and asymmetric hysteresis nonlinearities of piezoelectric actuators can be well estimated and compensated by the UDE-based controller without knowing the bound and shape. Different from those hysteresis existing in piezoelectric actuators, the hysteresis nonlinearities might be saturated in some actuators driven by other smart materials, e.g., magnetostrictive, shape memory alloys (SMA). In this section, the hysteresis loop of a SMA actuator characterized by the saturated GPI model is taken into consideration for the system (4). As identified in [9], the envelope functions are chosen to be $\gamma_L(v) = 22.271\tanh(0.0098v)$ and $\gamma_R(v) = 23.352\tanh(0.011v) + 2.279$. The density function is chosen to be $p(r_i) = 1.36e^{-0.21r_i}$ while the thresholds are $r_i = 0.86i$, $i = 0, 1, 2, 3, 4$. The hysteresis loop is given in Fig. 4 by using $v(t) = e^{-0.2t}(\sin(2\pi t)+1) - 0.7\,(^\circ\mathrm{C})$ as an excitation signal. For the tracking task, the desired trajectory is chosen as $x_m(t) = 40\cos(2\pi t)\ (mm)$ and the initial states of the system are set to be $\boldsymbol{X}(0) = [40\ 0]^T$. The simulation results are given in Fig. 5, from which, it can be seen that the tracking error is very small ($0.79mm$ with relative error 1.9%) and the lumped term is well estimated. This further demonstrates the extraordinary capability of UDE-based controller in handling the hysteresis uncertainty.

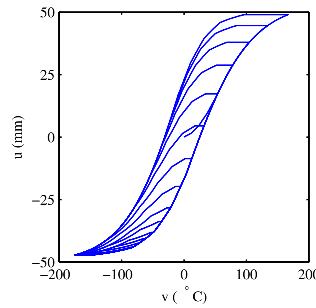

Figure 4. Saturated hysteresis loop.

VI. Conclusions

In this paper, the dynamics model of the piezoelectric actuator was identified as a second-order linear system preceded by the hysteresis characterized by the generalized Prandtl-Ishlinskii (GPI) model. Without the knowledge of the bound and shape of the hysteresis, the UDE-based controller was proposed and applied to piezoelectric actuator positioning control. The simulation results showed that both symmetric and asymmetric hysteresis uncertainties can be well estimated and compensated, and the trajectory tracking errors were all small enough to demonstrate the effectiveness of the proposed UDE-based controller. Further study on the saturated hysteresis effect compensation for SMA actuator was presented by using the UDE-based controller. In the future work, the experimental validation of the presented results will be conducted on a piezoelectric micropositioning stage from the Physik Instrumente Company.

References

[1] B. J. Kenton and K. K. Leang, "Design and control of a three-axis serial-kinematic high-bandwidth nanopositioner," *Mechatronics, IEEE/ASME Transactions on*, vol. 17, no. 2, pp. 356–369, 2012.

[2] Y. Li and Q. Xu, "Adaptive sliding mode control with perturbation estimation and PID sliding surface for motion tracking of a piezo-driven micromanipulator," *Control Systems Technology, IEEE Transactions on*, vol. 18, no. 4, pp. 798–810, 2010.

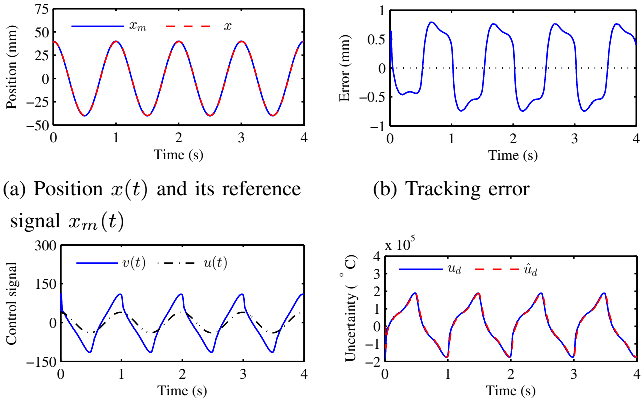

(a) Position $x(t)$ and its reference signal $x_m(t)$

(b) Tracking error

(c) Control signal $v(t)$ and hysteresis output $u(t)$

(d) Uncertainty $u_d(t)$ and its estimation $\hat{u}_d(t)$

Figure 5. Trajectory tracking performance of SMA actuator with saturated hysteresis.

[3] Y. Tian, B. Shirinzadeh, and D. Zhang, "A flexure-based mechanism and control methodology for ultra-precision turning operation," *Precision Engineering*, vol. 33, no. 2, pp. 160–166, 2009.

[4] M. Grossard, M. Boukallel, N. Chaillet, and C. Rotinat-Libersa, "Modeling and robust control strategy for a control-optimized piezoelectric microgripper," *Mechatronics, IEEE/ASME Transactions on*, vol. 16, no. 4, pp. 674–683, 2011.

[5] D. Zhang, D. G. Chetwynd, X. Liu, and Y. Tian, "Investigation of a 3-DOF micro-positioning table for surface grinding," *International Journal of Mechanical Sciences*, vol. 48, no. 12, pp. 1401–1408, 2006.

[6] A. J. Fleming and S. R. Moheimani, "Sensorless vibration suppression and scan compensation for piezoelectric tube nanopositioners," *Control Systems Technology, IEEE Transactions on*, vol. 14, no. 1, pp. 33–44, 2006.

[7] M. Karpelson, G.-Y. Wei, and R. J. Wood, "Driving high voltage piezoelectric actuators in microrobotic applications," *Sensors and Actuators A: Physical*, vol. 176, pp. 78–89, 2012.

[8] X. Chen and T. Hisayama, "Adaptive sliding-mode position control for piezo-actuated stage," *Industrial Electronics, IEEE Transactions on*, vol. 55, no. 11, pp. 3927–3934, 2008.

[9] M. Al Janaideh, S. Rakheja, and C.-Y. Su, "An analytical generalized Prandtl–Ishlinskii model inversion for hysteresis compensation in micropositioning control," *Mechatronics, IEEE/ASME Transactions on*, vol. 16, no. 4, pp. 734–744, 2011.

[10] R. H. Comstock, "Charge control of piezoelectric actuators to reduce hysteresis effects," Apr. 21 1981, uS Patent 4,263,527.

[11] C. Newcomb and I. Flinn, "Improving the linearity of piezoelectric ceramic actuators," *Electronics Letters*, vol. 18, no. 11, pp. 442–444, 1982.

[12] J. Minase, T.-F. Lu, B. Cazzolato, and S. Grainger, "A review, supported by experimental results, of voltage, charge and capacitor insertion method for driving piezoelectric actuators," *Precision Engineering*, vol. 34, no. 4, pp. 692–700, 2010.

[13] A. Fleming and S. Moheimani, "Precision current and charge amplifiers for driving highly capacitive piezoelectric loads," *Electronics Letters*, vol. 39, no. 3, pp. 282–284, 2003.

[14] A. J. Fleming and S. R. Moheimani, "Improved current and charge amplifiers for driving piezoelectric loads, and issues in signal processing design for synthesis of shunt damping circuits," *Journal of Intelligent Material Systems and Structures*, vol. 15, no. 2, pp. 77–92, 2004.

[15] S. Devasia, E. Eleftheriou, and S. R. Moheimani, "A survey of control issues in nanopositioning," *Control Systems Technology, IEEE Transactions on*, vol. 15, no. 5, pp. 802–823, 2007.

[16] G. Song, J. Zhao, X. Zhou, D. Abreu-Garcia *et al.*, "Tracking control of a piezoceramic actuator with hysteresis compensation using inverse Preisach model," *Mechatronics, IEEE/ASME Transactions on*, vol. 10, no. 2, pp. 198–209, 2005.

[17] L. Liu, K. K. Tan, S.-L. Chen, S. Huang, and T. H. Lee, "SVD-based Preisach hysteresis identification and composite control of piezo actuators," *ISA transactions*, vol. 51, no. 3, pp. 430–438, 2012.

[18] H. Jiang, H. Ji, J. Qiu, and Y. Chen, "A modified Prandtl-Ishlinskii model for modeling asymmetric hysteresis of piezoelectric actuators," *Ultrasonics, Ferroelectrics and Frequency Control, IEEE Transactions on*, vol. 57, no. 5, pp. 1200–1210, 2010.

[19] M. Al Janaideh, Y. Feng, S. Rakheja, C.-Y. Su, and C. A. Rabbath, "Hysteresis compensation for smart actuators using inverse generalized Prandtl-Ishlinskii model," in *American Control Conference, 2009. ACC'09.* IEEE, 2009, pp. 307–312.

[20] C.-Y. Su, Y. Feng, H. Hong, and X. Chen, "Adaptive control of system involving complex hysteretic nonlinearities: a generalised Prandtl–Ishlinskii modelling approach," *International Journal of Control*, vol. 82, no. 10, pp. 1786–1793, 2009.

[21] H. Sayyaadi and M. R. Zakerzadeh, "Position control of shape memory alloy actuator based on the generalized Prandtl–Ishlinskii inverse model," *Mechatronics*, vol. 22, no. 7, pp. 945–957, 2012.

[22] M. Rakotondrabe, "Bouc-Wen modeling and inverse multiplicative structure to compensate hysteresis nonlinearity in piezoelectric actuators." *Automation Science and Engineering, IEEE Transactions on*, vol. 8, no. 2, pp. 428–431, 2011.

[23] S. Bashash and N. Jalili, "A polynomial-based linear mapping strategy for feedforward compensation of hysteresis in piezoelectric actuators," *Journal of Dynamic Systems, Measurement, and Control*, vol. 130, no. 3, p. 031008, 2008.

[24] X. Tan and J. S. Baras, "Adaptive identification and control of hysteresis in smart materials," *Automatic Control, IEEE Transactions on*, vol. 50, no. 6, pp. 827–839, 2005.

[25] Y. Wu and Q. Zou, "Robust inversion-based 2-DOF control design for output tracking: piezoelectric-actuator example," *Control Systems Technology, IEEE Transactions on*, vol. 17, no. 5, pp. 1069–1082, 2009.

[26] C.-L. Hwang, "Microprocessor-based fuzzy decentralized control of 2-D piezo-driven systems," *Industrial Electronics, IEEE Transactions on*, vol. 55, no. 3, pp. 1411–1420, 2008.

[27] S. Duraiswamy and G.-C. Chiu, "Nonlinear adaptive nonsmooth dynamic surface control of electro-hydraulic systems," in *American Control Conference, 2003. Proceedings of the 2003*, vol. 4. IEEE, 2003, pp. 3287–3292.

[28] D. Le, B. W. Pietrzak, and G. M. Shaver, "Dynamic surface control of a piezoelectric fuel injector during rate shaping," *Control Engineering Practice*, vol. 30, pp. 12–26, 2014.

[29] Q.-C. Zhong and D. Rees, "Control of uncertain LTI systems based on an uncertainty and disturbance estimator," *Journal of dynamic systems, measurement, and control*, vol. 126, no. 4, pp. 905–910, 2004.

[30] B. Ren and Q.-C. Zhong, "UDE-based robust control for a class of non-affine nonlinear systems," in *ASME 2013 Dynamic Systems and Control Conference*. American Society of Mechanical Engineers, 2013, pp. V003T34A004–V003T34A004.

[31] G. Aguirre, T. Janssens, H. Van Brussel, and F. Al-Bender, "Asymmetric-hysteresis compensation in piezoelectric actuators," *Mechanical Systems and Signal Processing*, vol. 30, pp. 218–231, 2012.

[32] Q.-C. Zhong, A. Kuperman, and R. Stobart, "Design of UDE-based controllers from their two-degree-of-freedom nature," *International Journal of Robust and Nonlinear Control*, vol. 21, no. 17, pp. 1994–2008, 2011.